DeA- Ames

Final Technical Report NASA Grant NAGW-228
Principal Investigator, C. B. Leovy, University of Washington

Analysis of the Viking Lander 1 Surface Wind Vector for Sols 45 to 376

Summary of Project Approaches and Results

The purpose of this project was to find a means for correcting Viking Lander 1 wind sensor data during the period between sols 45 and 375. During this period, the heating element of the quadrant sensor which provided the primary signal used for determining wind direction had failed, but both hot film wind speed sensors were functioning normally. As a consequence the SANMET Program, used to provide wind speed and direction information, was not providing reliable results and an alternative procedure had to be developed.

The procedure which was tried and eventually adopted was as follows.

(1) The following information from the sensors was bin-averaged in 25 equal-sized bins per sol: Nusseldt numbers corrected for radiation effects determined separately for hot film wind speed sensors 1 and 2 (NU1, NU2), approximate wind speed determined only from these Nusseldt numbers (VQD, the error in the approximate determination relative to wind tunnel values is $\leq 5\%$ and was neglected), quadrant sensor thermocouple voltage differences (Q1, Q2, defined such that Q1>0 if thermocouple #1 had a higher temperature than thermocouple #2 and Q2>0 if thermocouple #3 had a higher temperature than thermocouple #3. See Fig. 1 for geometry of the wind sensor assembly. In addition, the number of data points per bin (typically ~100) was recorded.

(2) The function

$$F(\theta,VQD) = \frac{NU2-NU1}{(NU2-NU1)^{1/2}}$$

was evaluated for each bin. This function depends on wind direction with up to a 4-fold ambiguity. It also depends on wind speeds for winds below ~8 m/s, but only weakly. Calibration curves of F vs. wind direction θ, determined from SANMET for VL-1 sols prior to sol 45 and for selected VL-2 sols are shown in Fig. 2.

(3) Wind directions were divided into 12 sectors according to the values of F, Q1 and Q2 according to Table 1. Only the signs of F, A1, Q2, and $R = |Q1|/|Q2| - 1$ were used for this purpose. The sign groupings in Table 1 follow from the geometry (Fig. 1) for positive quadrant sensor post overheat. During the period of quadrant sensor heater failure, signals were observed on the quadrant sensor thermocouples at certain times of the day arising from radiative overheat or the quadrant sensor post relative to ambient air. Typically, clear cut signals occurred between 0800 and 1600 local time. During most of the remainder of most sols, the voltages were flat and slightly negative. These negative values were interpreted as bias voltages and had the values -.09mv (Q2) and -05mv (Q1). Before assessing the signs of Q1 and Q2 to be used in conjunction with Table 1, these biases were subtracted. If the resulting magnitude of Q1 or Q2 did not exceed .05 mv (our estimate of the random voltage noise, about 1 dn), it was taken to be a null value.

(4) During the portion of each sol when there was a null signal on Q1 or Q2, only the quadrant shown in Table 1 could be estimated a priori. This was done by using the continuity of the F signal in time: no change is sign of F implies no change in quadrant, a change in sign implies a change in quadrant. When a quadrant change occurred, judgment had to be exercised in order to determine whether the rotation was clockwise or counterclockwise. Moreover, within each quadrant as well as in sectors 1b, 2b, 3b, and 4b of Table 1, the directional solution is bimodal. For both of these problems, the time history of the F signal was used. If F passes through a single maximum since the last quadrant boundary crossing, the solution probably lies in the clockwise portion of the quadrant or sector. If F passes through no maximum or two maxima since the last sector crossing, the wind probably lies in the counterclockwise portion. This assessment requires judgment and carries an uncertainty, but the determinations were made easier because of certain observed properties of the signals which indicated that: (a) the dominant signal was a rather regular semidiurnal wind oscillation with clockwise rotation and (b) during the night, the wind pattern varied little from one night to the next. Fig. 3 illustrates a typical bin-averaged data set and the pattern of F, Q1, and Q2.

(5) After a sector or quadrant had been assigned to each bin and the assignment to clockwise or counterclockwise halves of the quadrants or "6"-sectors had also been made, a refined estimate of the wind direction using only F and the calibration curves of Fig. 2 was made on a point-by-point (not bin-average) basis, using the quadrant or sector assignment to select the correct solution from the set of up to 4 solutions for the same F values. Wind values were assigned to the appropriate peak in the F-curve for observed F values exceeding the peak. Examples of bin-average hodographs obtained in this way are shown in Fig. 4.

As a check, the procedure was applied to sols 20 and 21 are compared with the SANMET results for those sols. During this period, Q1 and Q2 signals provided sector information both day and night, however, the F signal was weaker and much noisier than during most of the period to which we have applied the technique. For this reason, we believe that the errors for these sols provide worst case estimates for the errors during sols 240-375 for which we have used this technique to reduce data. Figs. 4 and 5 show these comparisons. These results are also presented in Table 2 which gives the differences between bin-average wind directions derived in this way and those determined from SANMET. Differences are due primarily to the failure of the solution picked from the bin average sector to correspond to the point-by-point solution. This occurs most frequently during the afternoon convective period when wind direction is highly variable. Because Q1 and Q2 signals should exist during convective periods, this error could be reduced in the future by using the Q1 and Q2 signals to select sectors on a point-by-point rather than bin average basis during convective periods.

Despite these errors, the resulting wind direction estimates are quite satisfactory. The overall bin mean error magnitude for sols 20 and 21 is 14.6°, and is probably less in the actual data during autumn and winter when convection is weak and tidal winds strong and regular than it was in this test. These wind results have been used in the attached publication to help define the winter season meteorology at the VL-1 site and examples of the

resulting wind hodographs are shown in Figs. 6 and 7. We are currently extending the effort in two directions under another grant: (a) completing the reduction of wind data between sols 45 and 240 and, (b) using winds determined in this way to "calibrate" the quadrant sensor signals (during the daytime), so that these signals can be used by themselves to determine wind direction after the failure of one of the hot film wind sensors on sol 375.

Reference

Leovy, C. B., J. M. Tillman, W. R. Guest, and J. R. Barnes, 1984: Interannual variability of Martian Weather. Proceeding of Seymour Hess Symposium, IAMAP, Cambridge University Press (in press).

Quadrant	Sector	Angle Range	F	Q1	Q2	R	Remarks
1	1a	012-035	F>0	Q1<0	Q2>0	R<0	-
1	1b	035-057	F>0	Q1<0	Q2>0	R>0	counterclockwise sector half, R small
1	1b	057-080	F>0	Q1<0	Q2>0	R>0	clockwise sector half, R large
1	1c	080-102	F>0	Q1<0	Q2<0	R>0	-
2	2a	102-125	F<0	Q1<0	Q2<0	R<0	-
2	2b	125-147	F<0	Q1<0	Q2<0	R<0	counterclockwise sector half, R small
2	2b	147-170	F<0	Q1<0	Q2<0	R<0	clockwise sector half, R large
2	2c	170-192	F<0	Q1>0	Q2<0	R<0	-
3	3a	192-215	F>0	Q1>0	Q2<0	R<0	-
3	3b	215-237	F>0	Q1>0	Q2<0	R>0	counterclockwise sector half, R small
3	3b	237-260	F>0	Q1>0	Q2<0	R>0	clockwise sector half, R large
3	3c	260-292	F>0	Q1>0	Q2>0	R>0	-
4	4a	292-305	F<0	Q1>0	Q2>0	R>0	-
4	4b	305-327	F<0	Q1<0	Q2>0	R<0	counterclockwise sector half, R small
4	4b	327-350	F<0	Q1<0	Q2>0	R<0	clockwise sector half, R large
4	4c	350-012	F<0	Q1<0	Q2>0	R<0	-

Table 1. Sector nomenclature and relationships between wind-sensor assembly signals, sectors, and angles.

Bin	Time of Day (fraction of sol)	Difference (deg)	Time of day (fraction of sol)	Difference (deg)
1	20.02	- 2.7	21.02	- 9.5
2	20.06	- 2.6	21.06	- 4.9
3	20.10	- 4.6	21.10	- 0.1
4	20.14	- 4.3	21.14	- 3.6
5	20.18	+ 6.1	21.18	- 4.8
6	20.22	- 5.9	21.22	- 4.9
7	20.26	- 0.2	21.26	- 9.3
8	20.30	+18.2	21.30	+ 0.8
9	20.34	+12.9	21.34	- 8.0
10	20.38	-15.4	21.38	-12.1
11	20.42	- 7.9	21.42	+ 1.5
12	20.46	- 3.5	21.46	-
13	20.50	+11.4	21.50	+11.0
14	20.54	+ 2.6	21.54	+14.9
15	20.58	+22.0	21.58	+15.9
16	20.62	+12.4	21.62	+ 9.3
17	20.66	- 7.4	21.66	- 8.6
18	20.70	+22.9	21.70	- 4.8
19	20.74	+ 7.4	21.74	- 6.7
20	20.78	+ 4.5	21.78	- 4.9
21	20.82	+ 5.1	21.82	-13.3
22	20.86	-27.2	21.86	-40.6
23	20.90	- 7.8	21.90	+ 2.3
24	20.94	+ 5.6	21.94	+ 4.1
25	20.98	-18.8	21.98	- 5.9

Table 2: Differences (in degrees) between bin average directions calculated from the wind sensor only and those calculated by SANMET.

Figure Legends

Fig. 1 Geometry of Lander 1 wind sensors relative to directional coordinates on Mars. Notation: TC - wind direction sensor thermocouple, ws - hot film wind sensor.

Fig. 2 Calibration curves for F derived from a combination of data from VL-1 prior to sol 45 and VL-2 data.

Fig. 3. Example of bin average data for Q1, Q2 and F for VL-1 sol 246.

Fig. 4 Technique test results, VL-1 sol 20. Wind sensor only wind direction (ANSWS, derived as described in the text) are compared with wind directions determined by SANMET. Error bars represent the standard deviation of the difference between ANGWS and SANMET winds.

Fig. 5 Same as Fig. 4, except for VL-1 sol 21.

Fig. 6 Example hodographs for VL-1 derived by the wind sensor only technique (ANGWS). Sol number (upper right) and LS value (upper left, parentheses) are given.

Fig. 7 Same as Fig. 6, but for VL-1 sol 320.

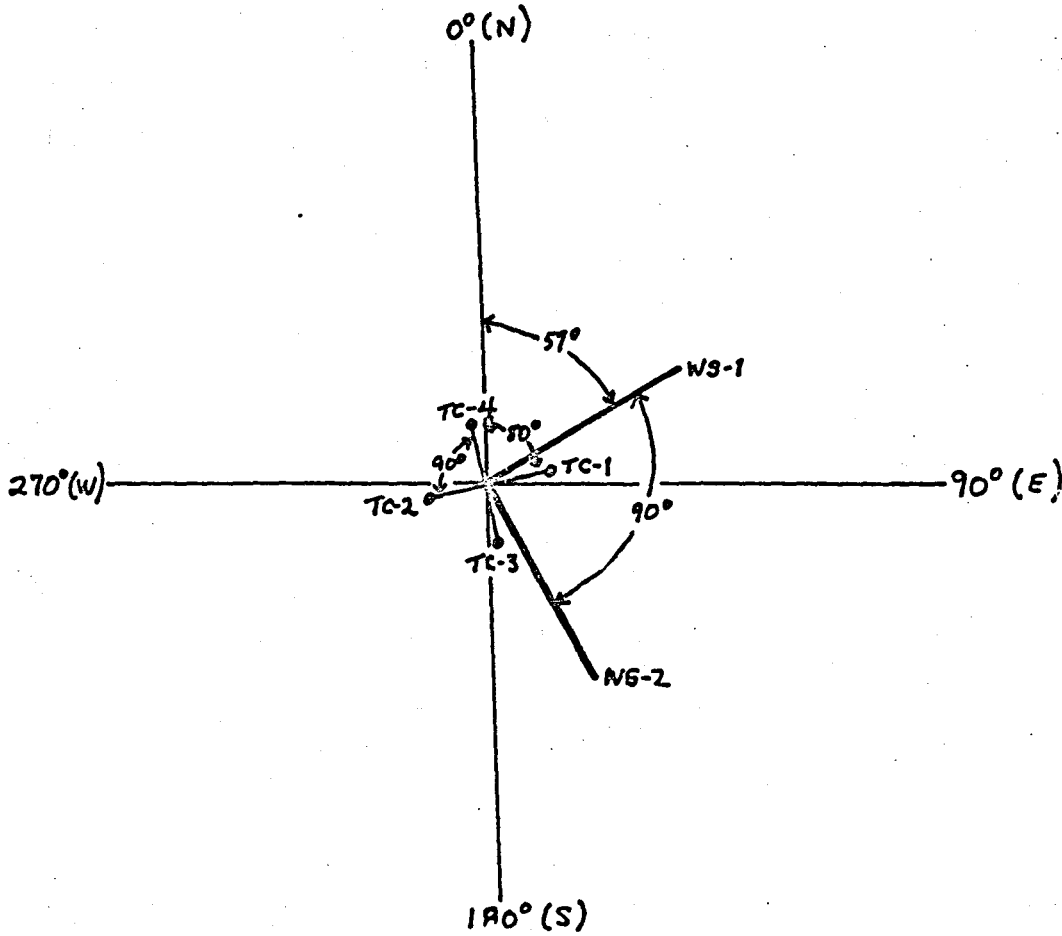
0° (N)
57°
WS-1
TC-4
80°
90°
TC-1
270° (W)
TC-2
90° (E)
90°
TC-3
NS-2
180° (S)

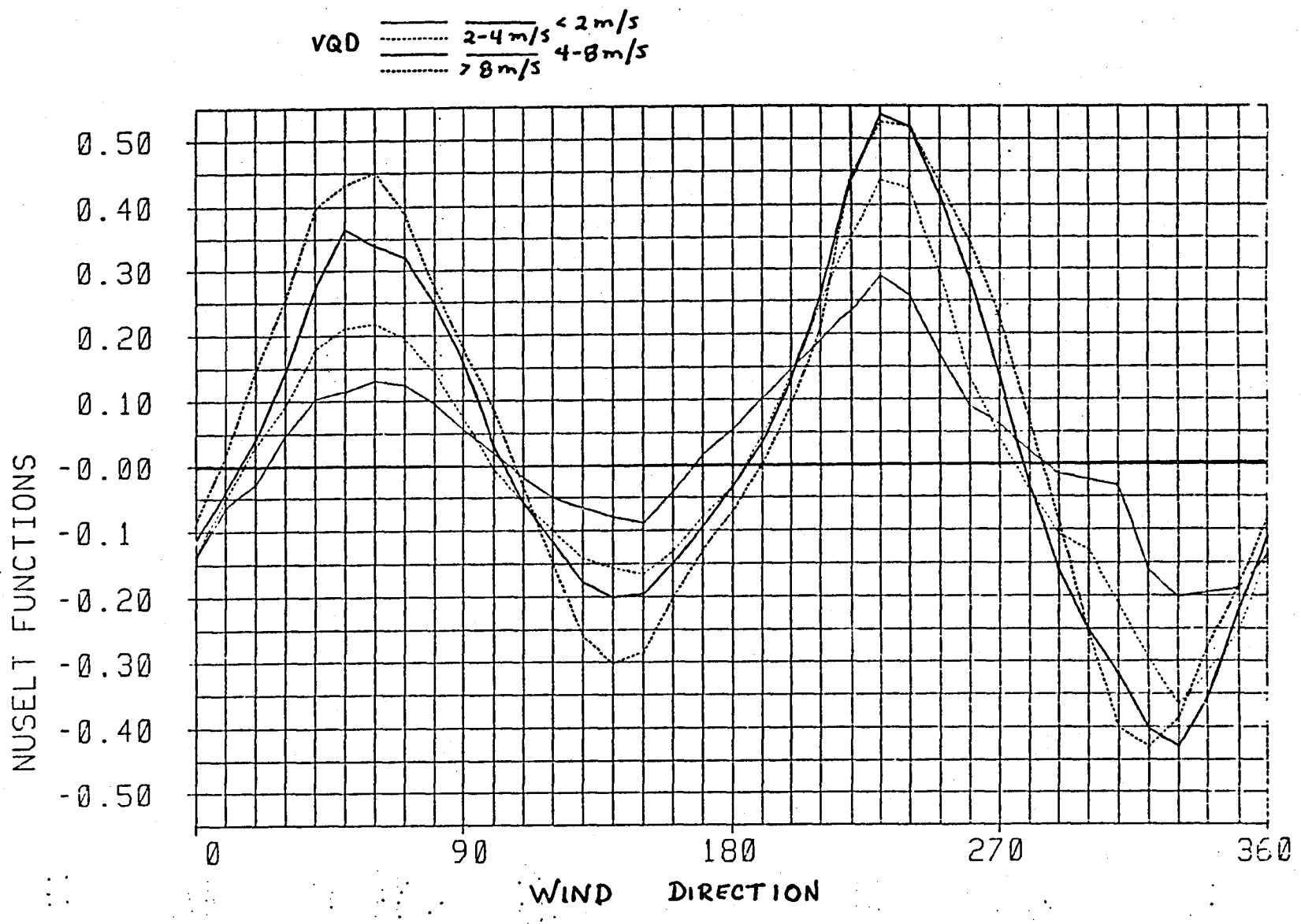
VQD
< 2 m/s
2-4 m/s
4-8 m/s
> 8 m/s
0.50
0.40
0.30
0.20
0.10
-0.00
-0.1
-0.20
-0.30
-0.40
-0.50
NUSELT FUNCTIONS
0
90
180
270
360
WIND DIRECTION

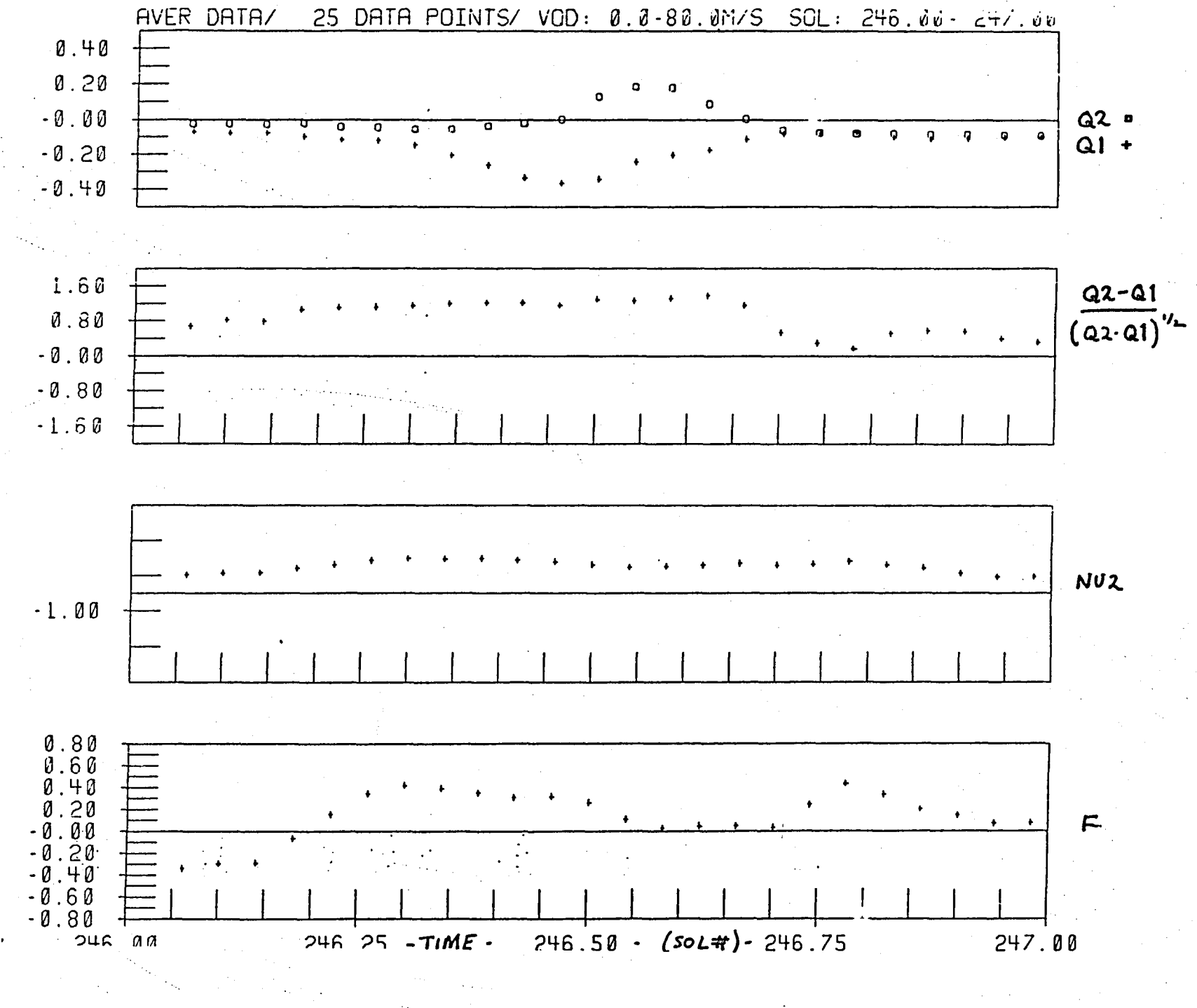
AVER DATA/ 25 DATA POINTS/ VOD: 0.0-80.0M/S SOL: 246.00- 247.00
0.40
0.20
-0.00
-0.20
-0.40
Q2 ▫
Q1 +
1.60
0.80
-0.00
-0.80
-1.60
Q2-Q1
(Q2·Q1)^1/2
-1.00
NU2
0.80
0.60
0.40
0.20
-0.00
-0.20
-0.40
-0.60
-0.80
F
246.00
246.25 -TIME-
246.50 - (SOL#)-
246.75
247.00

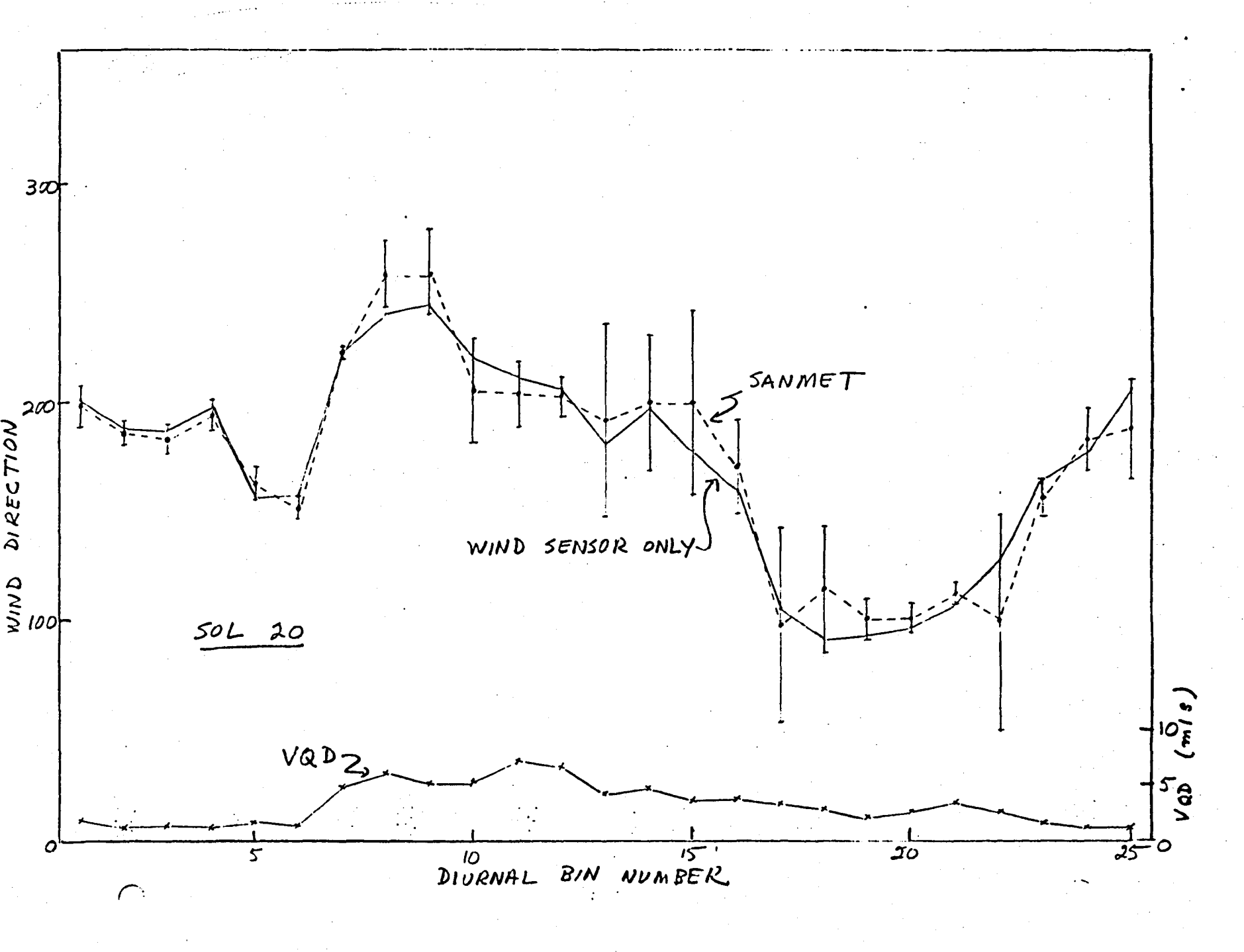
300
200
100
0
WIND DIRECTION
SANMET
WIND SENSOR ONLY
SOL 20
VQD2
5
10
15
20
25
DIURNAL BIN NUMBER
10
5
0
VQD (m/s)

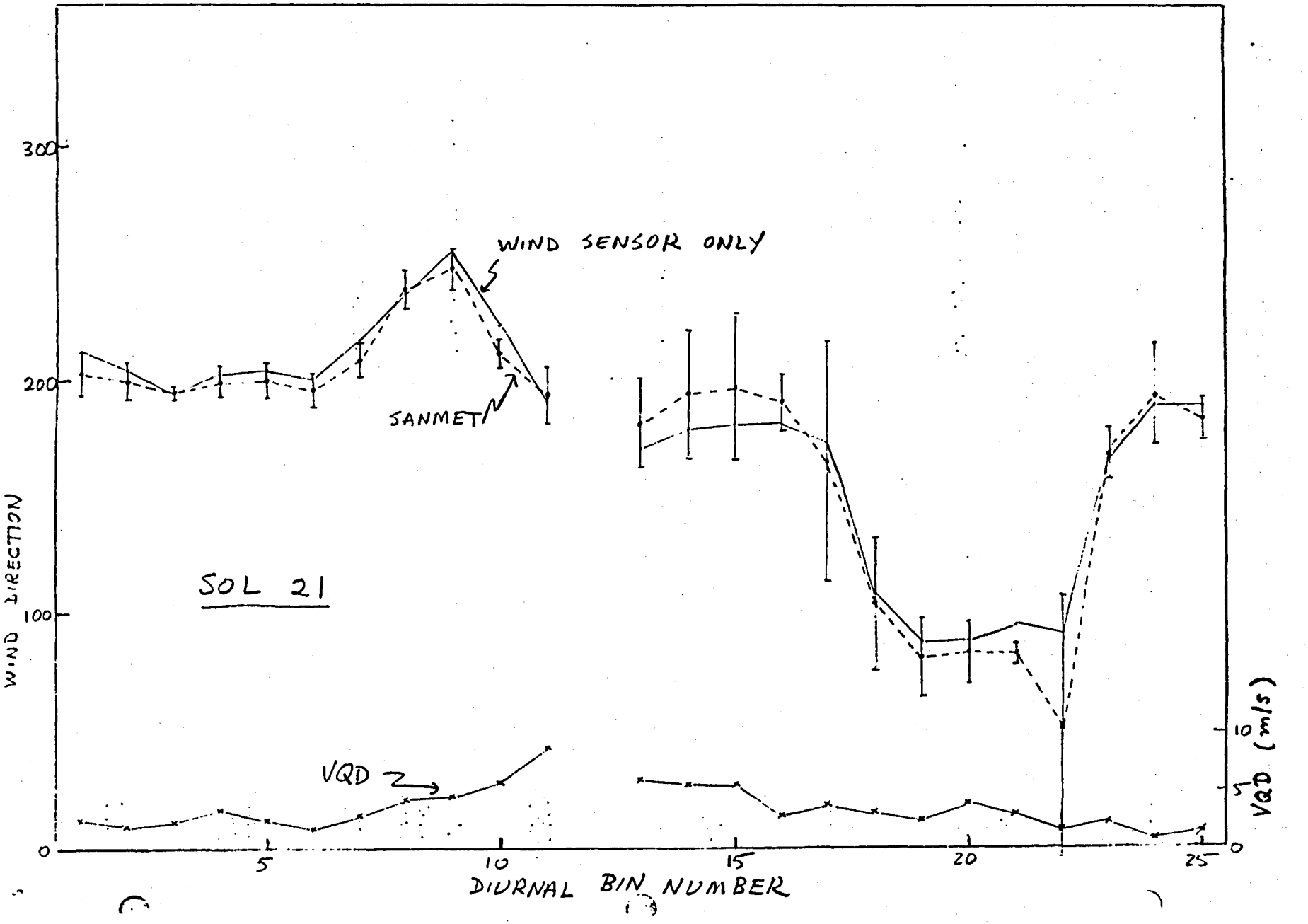
300
200
100
0
WIND SENSOR ONLY
SANMET
SOL 21
VQD
WIND DIRECTION
VQD (m/s)
10
5
0
5
10
15
20
25
DIURNAL BIN NUMBER

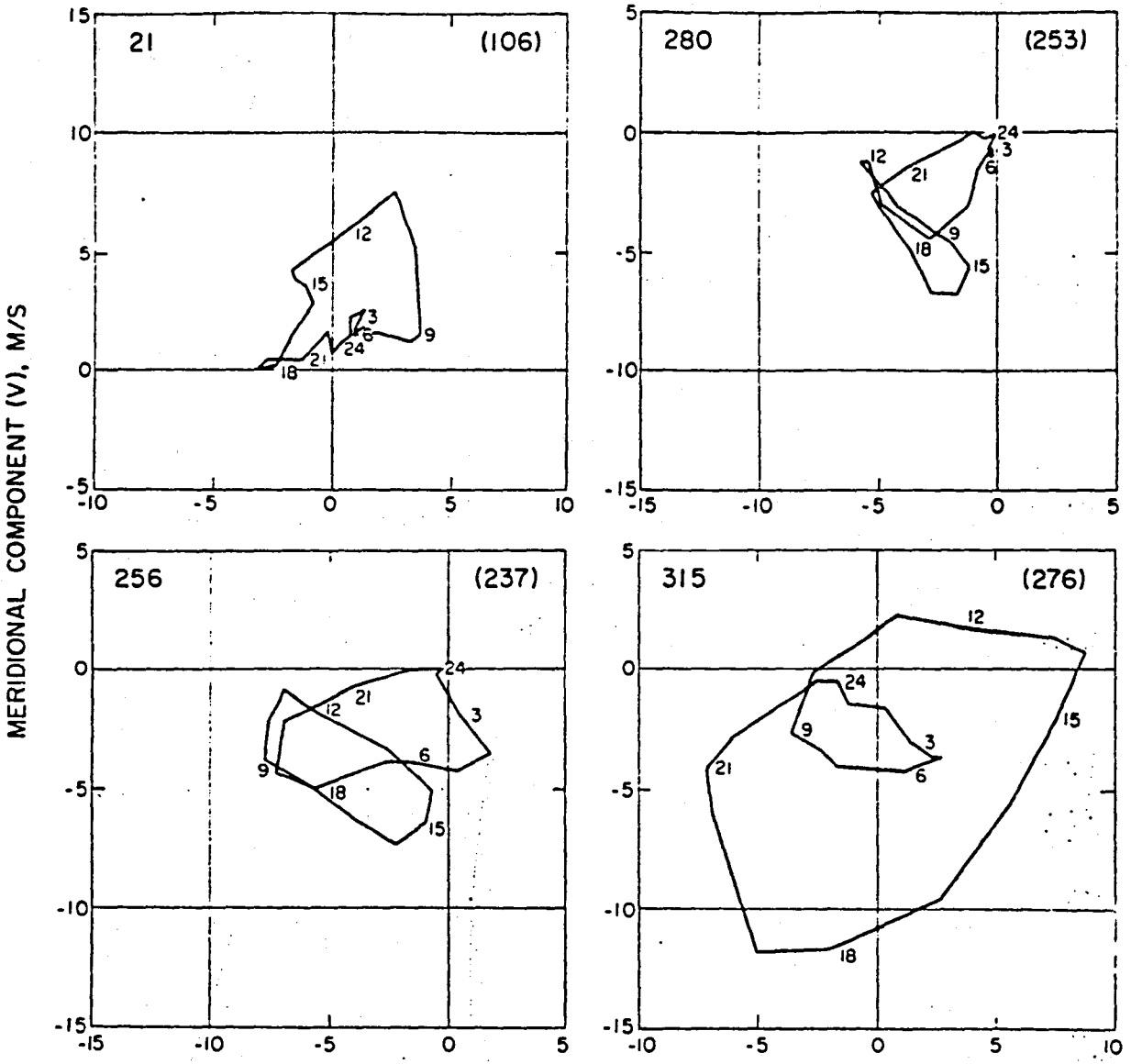

LANDER I HODOGRAPHS

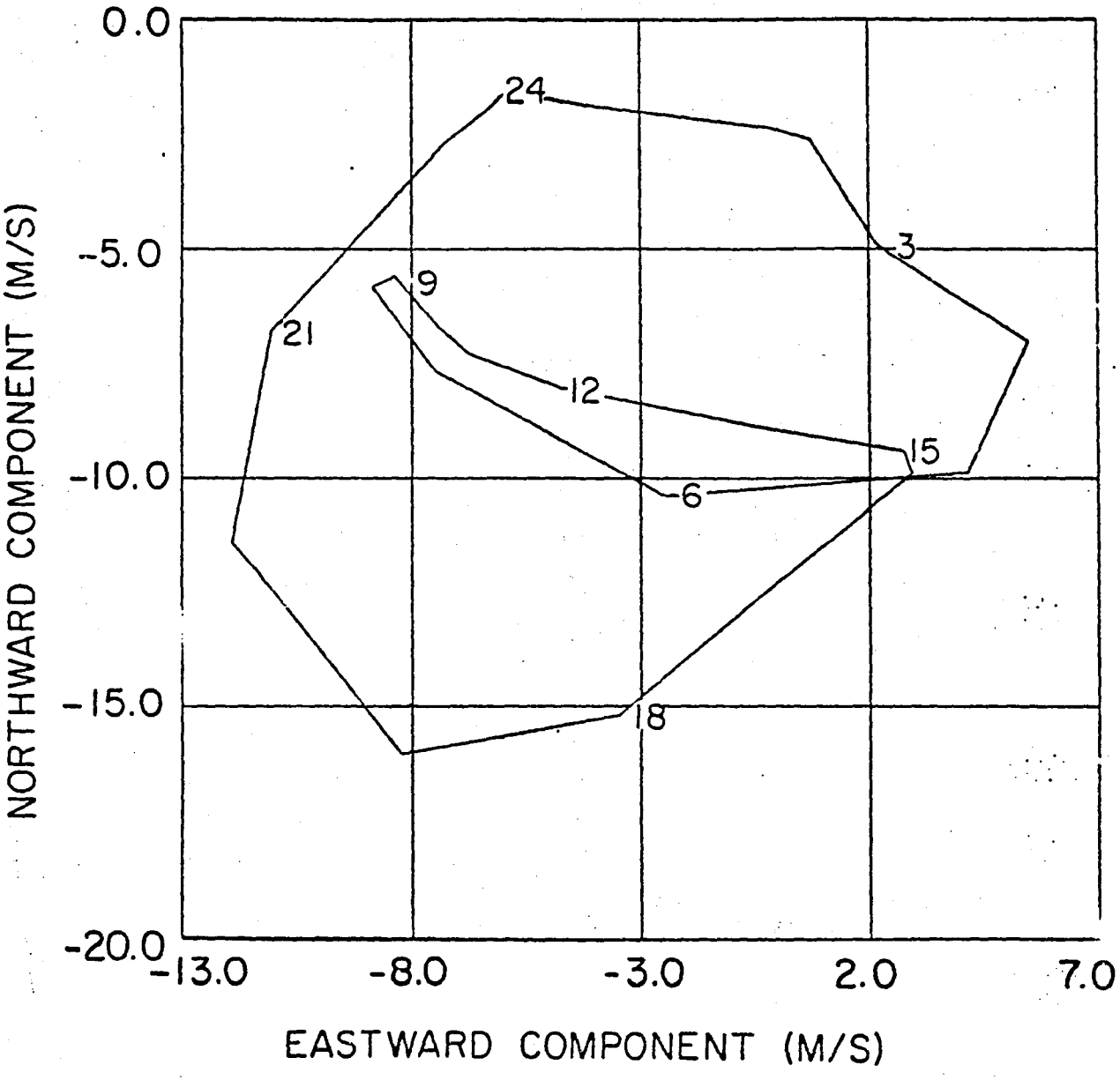
0.0
-5.0
-10.0
-15.0
-20.0
-13.0
-8.0
-3.0
2.0
7.0
NORTHWARD COMPONENT (M/S)
EASTWARD COMPONENT (M/S)
24
3
9
21
12
15
6
18

END

DATE

FILMED

APR 12 1985

End of Document